Identification of important residues of insulin-like peptide 5 and its receptor RXFP4 for ligand–receptor interactions

ARTICLE *in* ARCHIVES OF BIOCHEMISTRY AND BIOPHYSICS · SEPTEMBER 2014

Impact Factor: 3.02 · DOI: 10.1016/j.abb.2014.07.010

6 AUTHORS, INCLUDING:

Zhan-Yun Guo
Tongji University
61 PUBLICATIONS **587** CITATIONS

SEE PROFILE

Archives of Biochemistry and Biophysics 558 (2014) 127–132

Contents lists available at ScienceDirect

Archives of Biochemistry and Biophysics

journal homepage: www.elsevier.com/locate/yabbi

Identification of important residues of insulin-like peptide 5 and its receptor RXFP4 for ligand–receptor interactions

Xin-Yi Wang [a,b], Yu-Qi Guo [a], Xiao-Xia Shao [a], Ya-Li Liu [b], Zeng-Guang Xu [b], Zhan-Yun Guo [a,b,*]

[a] Institute of Protein Research, College of Life Sciences and Technology, Tongji University, Shanghai 200092, China
[b] Central Laboratory, Shanghai East Hospital, Tongji University School of Medicine, Shanghai 200120, China

ARTICLE INFO

Article history:
Received 8 June 2014
and in revised form 4 July 2014
Available online 18 July 2014

Keywords:
INSL5
RXFP4
Ligand–receptor interaction
Electrostatic interaction
Mutagenesis

ABSTRACT

Insulin-like peptide 5 (INSL5) is an insulin/relaxin superfamily peptide involved in the regulation of glucose homeostasis by activating its receptor RXFP4, which can also be activated by relaxin-3 in vitro. To determine the interaction mechanism of INSL5 with its receptor RXFP4, we studied their electrostatic interactions using a charge-exchange mutagenesis approach. First, we identified three negatively charged extracellular residues (Glu100, Asp104 and Glu182) in human RXFP4 that were important for receptor activation by wild-type INSL5. Second, we demonstrated that two positively charged B-chain Arg residues (B13Arg and B23Arg) in human INSL5 were involved in receptor binding and activation. Third, we proposed probable electrostatic interactions between INSL5 and RXFP4: the B-chain central B13Arg of INSL5 interacts with both Asp104 and Glu182 of RXFP4, meanwhile the B-chain C-terminal B23Arg of INSL5 interacts with both Glu100 and Asp104 of RXFP4. The present electrostatic interactions between INSL5 and RXFP4 were similar to our previously identified interactions between relaxin-3 and RXFP4, but had subtle differences that might be caused by the different B-chain C-terminal conformations of relaxin-3 and INSL5 because a dipeptide exchange at the B-chain C-terminus significantly decreased the activity of INSL5 and relaxin-3 to receptor RXFP4.

Introduction

Insulin-like peptide 5 (INSL5,[1] also known as RIF2) is an insulin/relaxin superfamily peptide hormone first identified in 1999 [1–4]. It is primarily expressed in the rectum, colon and uterus [3,4]. INSL5 is the endogenous agonist of the relaxin family peptide receptor RXFP4, formerly known as orphan G protein-coupled receptor GPCR142 [5]. In vitro, RXFP4 can also be activated by the neuropeptide relaxin-3 (also known as INSL7), whose cognate receptor is the homologous RXFP3 [6]. A recent gene knockout experiment demonstrated that INSL5 is involved in the regulation of glucose homeostasis in mice [7]. Thus, INSL5/RXFP4 system may be a potential therapeutic target for diabetes.

In recent studies, electrostatic interactions of relaxin-3 with both RXFP3 and RXFP4 have been identified, and involve three highly conserved positively charged B-chain Arg residues (B12Arg, B16Arg and B16Arg) of relaxin-3 and a highly conserved negatively charged EXXXD motif of both receptors [8–10]. To test whether INSL5 and relaxin-3 activate receptor RXFP4 through a similar mechanism, we studied the electrostatic interactions between INSL5 and RXFP4 using a charge-exchange mutagenesis approach. Our present results showed that the electrostatic interactions between INSL5 and its receptor RXFP4 were similar to those between relaxin-3 and RXFP4, but had subtle differences that might be caused by the different B-chain C-terminal conformations of relaxin-3 and INSL5.

Experimental methods

Site-directed mutagenesis and recombinant preparation of mutant INSL5s

The expression constructs of mutant INSL5s were generated by site-directed mutagenesis using the QuikChange approach. An expression construct of a designed single-chain human INSL5 precursor was used as the mutagenesis template [11]. The expected mutations were confirmed by DNA sequencing. The mutant INSL5 precursors were recombinantly expressed in *Escherichia coli*, refolded in vitro, and converted to the two-chain mature form

* Corresponding author at: Institute of Protein Research, College of Life Sciences and Technology, Tongji University, 1239 Siping Road, Shanghai 200092, China. Fax: +86 21 65988403.
E-mail address: zhan-yun.guo@tongji.edu.cn (Z.-Y. Guo).

[1] *Abbreviations used:* INSL5, insulin-like peptide 5; CRE, cAPM response element; HEK293T, human embryonic kidney 293T; RP-HPLC, reverse-phase high performance liquid chromatography; TMD, transmembrane domain.

http://dx.doi.org/10.1016/j.abb.2014.07.010
0003-9861/

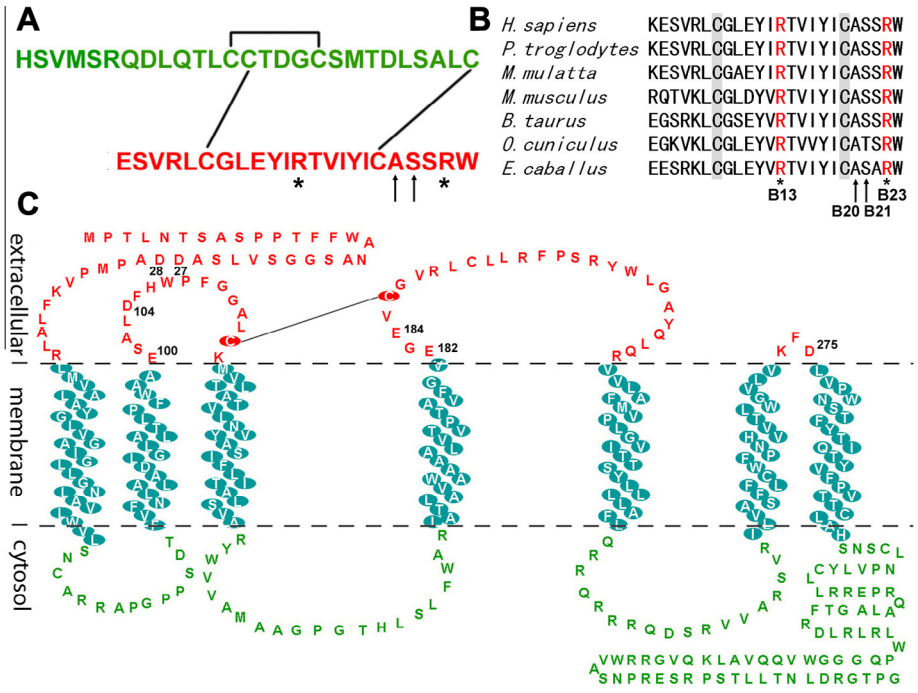

Fig. 1. (A) The amino acid sequence of the recombinant human INSL5. The A-chain is shown in green and B-chain in red. Lines indicate disulfide linkages. Asterisks indicate the two conserved B-chain Arg residues. Arrows indicate the B-chain C-terminal residues determined the C-terminal conformation. (B) The amino acid sequence alignment of the INSL5 B-chains from different species. The highly conserved B-chain arginine residues are shown in red. (C) The predicted membrane topology of human RXFP4. The negatively charged residues in the extracellular domain were labeled and replaced by positively charged arginine, respectively. TMHMM Server v.2.0 (www.cbs.dtu.dk/services/TMHMM/) and TMpred Server (http://www.ch.embnet.org/cgi-bin/TMPRED) predicted the transmembrane topology of RXFP4, which generated a relatively consistent model with seven transmembrane domains. (For interpretation of the references to color in this figure legend, the reader is referred to the web version of this article.)

according to our previously published procedure [11]. The mutant INSL5s were purified to homogeneity using C_{18} reverse-phase high performance liquid chromatography (RP-HPLC) and their molecular masses were measured by mass spectroscopy.

Circular dichroism analysis

The mature wild-type and mutant INSL5s were dissolved in 1.0 mM aqueous HCl solution (pH3.0), respectively. Their concentrations were determined by ultraviolet absorbance at 280 nm using an extinction coefficient of $\varepsilon_{280nm} = 8480\ M^{-1}\ cm^{-1}$, which was calculated from the number of tryptophan and tyrosine residues in the peptides. Their final concentrations were adjusted to 20 μM for circular dichroism measurement, which was performed on a Jasco-715 spectrometer at room temperature. The spectra were scanned from 250 nm to 190 nm using a quartz cuvette with a 0.1 cm path length.

Receptor binding assays

The competition receptor-binding assays were carried out according to our previous procedure using a DTPA/Eu^{3+}-labeled chimeric R3/I5 peptide as a tracer [12]. Briefly, transfected human embryonic kidney 293T (HEK293T) cells, transiently overexpressing wild-type human RXFP4, were seeded into a 96-well plate and continuously cultured at 37 °C until they reached approximately 90% confluence (24–48 h). For the receptor-binding assays, the culture medium was removed and the binding solution (serum-free DMEM medium plus 1% bovine serum albumin, 200 μl/well) containing 4.0 nM of DTPA/Eu^{3+}-labeled R3/I5 tracer and different concentrations of wild-type or mutant INSL5 was added. After binding at 21–22 °C for 2 h, the binding solution was removed and the cells were washed twice with cold serum-free DMEM medium (200 μl/well). Enhancer solution (from Perkin-Elmer, Waltham, MA, USA, 100 μl/well) was then added to dissociate Eu^{3+} from the DTPA chelator. After shaking for 1–2 h, the solutions (80 μl/well) were transferred to a white opaque 384-well plate for time-resolved fluorescence measurement using a SpectraMax M5 plate reader (Molecular Devices, Sunnyvale, CA, USA). Nonspecific binding was determined by competition with 1.0 μM of wild-type INSL5. The specific binding data were fitted to sigmoidal curves, $Y = 100/(1 + 10^{X-\log IC50})$, using SigmaPlot 10.0 software.

Receptor activation assays

Receptor activation assays were carried out using a CRE-controlled nanoluciferase as the reporter [10]. The expression construct of wild-type or mutant RXFP4 (pcDNA6/RXFP4) and the reporter vector (pNL1.2/CRE) were co-transfected into HEK293T cells. One day after transfection, the cells were trypsinized and seeded into a 96-well plate. After the cells grew to ~90% confluence (24–48 h), the medium was removed and the activation solution (serum-free DMEM medium plus 1% bovine serum albumin, 100 μl/well) containing 5 μM of forskolin and different concentrations of wild-type or mutant INSL5 was added. After the cells were continuously cultured at 37 °C for 5–6 h, the activation solution was removed and the cells were lysed using lysis solution (Promega, Madison, WI, USA, 100 μl/well). Thereafter, the cell lysate (50 μl/well) was transferred to a white opaque 96-well plate. After addition of the 50-fold diluted nanoluciferase substrate (Promega, diluted in phosphate buffered saline, 50 μl/well), the bioluminescence was immediately measured on a SpectraMax M5 plate reader (Molecular Devices) using the luminescence mode. The relative bioluminescence data were fitted to sigmoidal curves, $Y = \min + (100-\min)/(1 + 10^{X-\log EC50})$, using SigmaPlot 10.0 software.

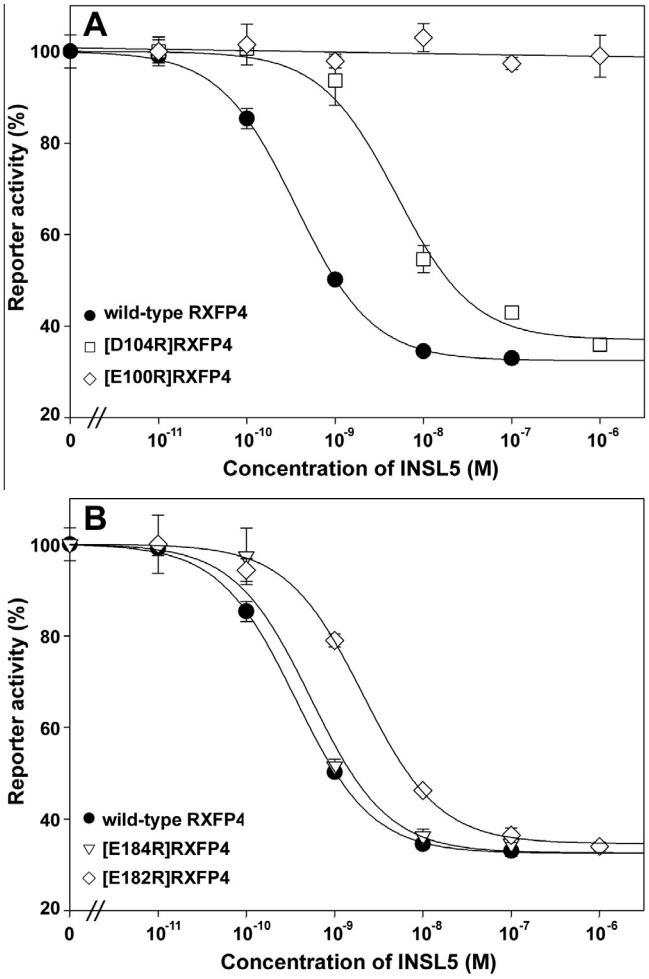

Fig. 2. Activation of the wild-type and mutant RXFP4s by wild-type INSL5. A CRE-controlled nanoluciferase reporter was used in these assays. The relative reporter activities were expressed as mean ± SE (n = 3) and fitted with sigmoidal curves using the SigmaPlot 10.0 software.

Table 1
The measured pEC50 values of wild-type INSL5 towards wild-type and mutant RXFP4s. The pEC50 values were calculated from receptor-activation assays that used a CRE-controlled nanoluciferase as the reporter. The data are expressed as mean ± SE (n = 3). N.D., not detectable.

RXFP4s	pEC50
Wild-type	9.46 ± 0.06
D27R	9.75 ± 0.23
D28R	9.67 ± 0.05
E100R	N.D.
D104R	8.30 ± 0.09
E182R	8.69 ± 0.16
E184R	9.27 ± 0.11
D275R	9.41 ± 0.15

Results and discussion

Identification of the negatively charged extracellular residues important for RXFP4 activation by INSL5

In a recent study [10], we replaced the negatively charged extracellular residues of human RXFP4 with positively charged arginine to identify the residues important for RXFP4 activation by relaxin-3 (Fig. 1). INSL5 is the endogenous ligand of RXFP4, thus in the present work, we attempted to identify the residues important for RXFP4 activation by INSL5 using these previously generated mutant RXFP4s (Fig. 2; the calculated pEC50 values are summarized in Table 1). When Glu100 was replaced by Arg, the mutant RXFP4 completely lost its response to wild-type INSL5 in the receptor activation assay, although it could be activated by high concentrations of relaxin-3 and was normally trafficked to the cell membrane, as shown in our previous work [10]. When Asp104 of RXFP4 was replaced by Arg, the sensitivity of the mutant receptor to wild-type INSL5 was significantly decreased (by over 10-fold). When Glu182 of RXFP4 was replaced by Arg, the sensitivity of the mutant receptor to wild-type INSL5 was moderately decreased (by ~6-fold). Other mutant RXFP4s retained almost normal sensitivity to wild-type INSL5. Thus, we deduced that the negatively charged Glu100, Asp104 and Glu182 of human RXFP4 are involved in the interaction with INSL5. Among them, Glu100 and Asp104 are located in a highly conserved EXXXD motif at the extracellular end of the second predicted transmembrane domain (TMD2), and Glu182 is at the extracellular end of TMD3. Thus, they are probably adjacent in the tertiary structure of RXFP4 and are involved in electrostatic interactions with INSL5.

Importance of the conserved positively charged B-chain Arg residues of INSL5

In previous studies, we demonstrated that three conserved positively charged B-chain Arg residues (B12Arg, B16Arg and B26Arg) of human relaxin-3 were important for binding and activation of both RXFP3 and RXFP4 [9,10]. INSL5 contains two highly conserved positively charged Arg residues in the B-chain, B13Arg and B23Arg, which correspond to B16Arg and B26Arg of relaxin-3, respectively (Fig. 1). To test their importance, we replaced B13Arg and B23Arg of human INSL5 with a negatively charged Glu residue, respectively. Single-chain precursors of the mutant INSL5s were overexpressed in *E. coli* and refolded in vitro. After treatment by endoproteinase Lys-C and carboxypeptidase B, mature two-chain mutant INSL5s were obtained with a yield similar to that of wild-type INSL5. Mass spectrometry analysis confirmed that the mutant INSL5s had the correct molecular mass (Table 2). The secondary structure of the mutant INSL5s was assessed by circular dichroism spectroscopy (Fig. 3A): the spectra of both mutants were quite similar to that of the wild-type INSL5, suggesting that mutation of B13Arg or B23Arg caused little structural disturbance to INSL5. However, mutation of B13Arg or B23Arg caused serious detriment to the function of INSL5 (Fig. 3B and C): their

Table 2
The measured molecular masses, pEC50 and pIC50 values of INSL5 mutants used in the present work.

INSL5s	Wild-type	B13E	B23E	B20G, B21G
Molecular mass[a]	5632.0 (5631.5)	5604.0 (5604.4)	5604.3 (5604.4)	5588.0 (5587.5)
pEC50[b]	9.46 ± 0.06	8.27 ± 0.21	~6	8.62 ± 0.07
pIC50[c]	7.47 ± 0.04	6.77 ± 0.05	N.D.[d]	6.17 ± 0.05

[a] The theoretical values are shown in the parentheses.
[b] Activation of wild-type human RXFP4.
[c] Binding with wild-type human RXFP4.
[d] N.D., not detectable.

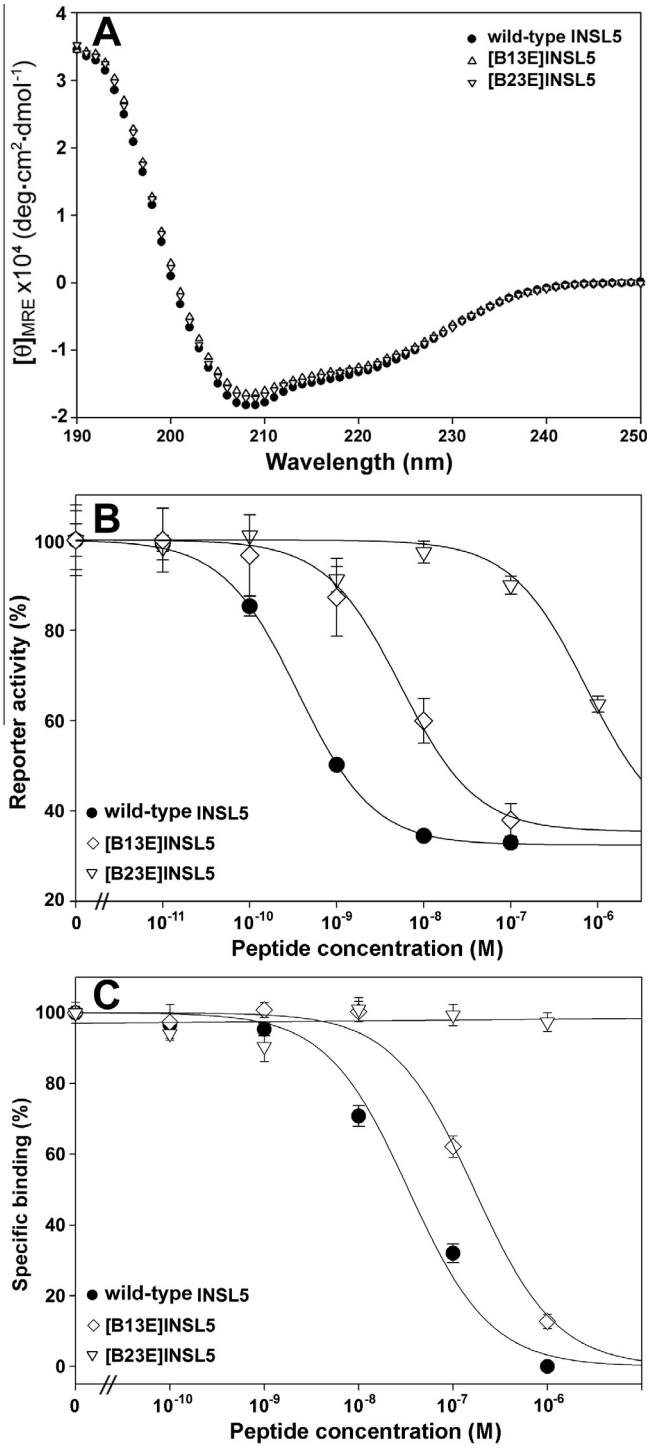

Fig. 3. Characterization of the mutant INSL5s carrying an Arg to Glu mutation. (A) Circular dichroism spectra. (B) Activation of the wild-type RXFP4. A CRE-controlled nanoluciferase was used as the reporter. The relative reporter activities were expressed as mean ± SE (n = 3) and fitted with sigmoidal curves using SigmaPlot 10.0 software. (C) Binding with the wild-type RXFP4. A europium-labeled R3/I5 peptide was used as the tracer. The specific binding data were expressed as mean ± SE (n = 3) and fitted with sigmoidal curves using SigmaPlot 10.0 software.

receptor-binding and receptor-activation potencies towards wild-type RXFP4 were significantly decreased, especially the B23Arg mutant. Thus, we deduced that B13Arg and B23Arg of INSL5 are involved in the interaction with RXFP4, especially the B-chain C-terminal B23Arg.

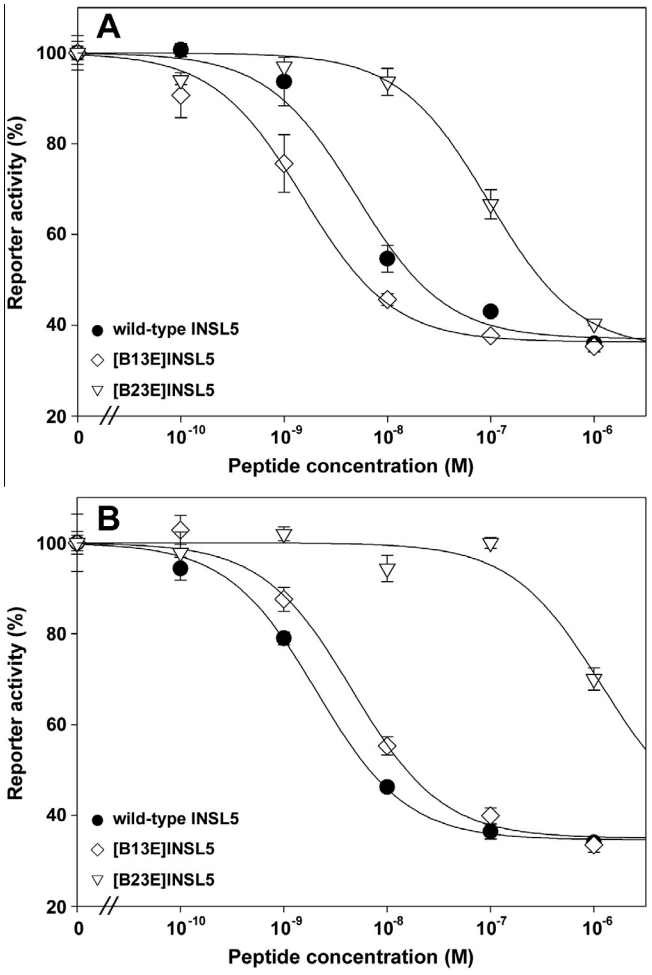

Fig. 4. Activation of [D104R]RXFP4 (A) and [E182R]RXFP4 (B) by wild-type and mutant INSL5s. A CRE-controlled nanoluciferase was used as the reporter in these assays. The data were expressed as mean ± SE (n = 3) and fitted with sigmoidal curves using SigmaPlot 10.0 software.

Table 3
The measured pEC50 values of the wild-type and mutant INSL5s towards the wild-type and mutant RXFP4s. The pEC50 values were calculated from receptor-activation assays that used a CRE-controlled nanoluciferase as the reporter. The data are expressed as mean ± SE (n = 3). N.D., not detectable.

Receptor RXFP4s	INSL5s		
	Wild-type	B13E	B23E
Wild-type	9.46 ± 0.06	8.27 ± 0.21	~6
E100R	N.D.	N.D.	N.D.
D104R	8.30 ± 0.09	8.82 ± 0.10	7.02 ± 0.08
E182R	8.69 ± 0.16	8.34 ± 0.09	~6

Probable electrostatic interaction pairs between INSL5 and RXFP4

The above results revealed three important negatively charged residues (Glu100, Asp104 and Glu182) in RXFP4 and two important positively charged residues (B23Arg and B13Arg) in INSL5. Subsequently, we attempted to identify the probable interaction pairs between these oppositely charged residues, according to the activity complementation between the mutant ligands and the mutant receptors. For [D104R]RXFP4, activation by [B13E]INSL5 was more effective than that of wild-type INSL5 (Fig 4A; the calculated pEC50 values are summarized in Table 3), suggesting that B13Arg of INSL5 probably interacts with Asp104 of RXFP4 during

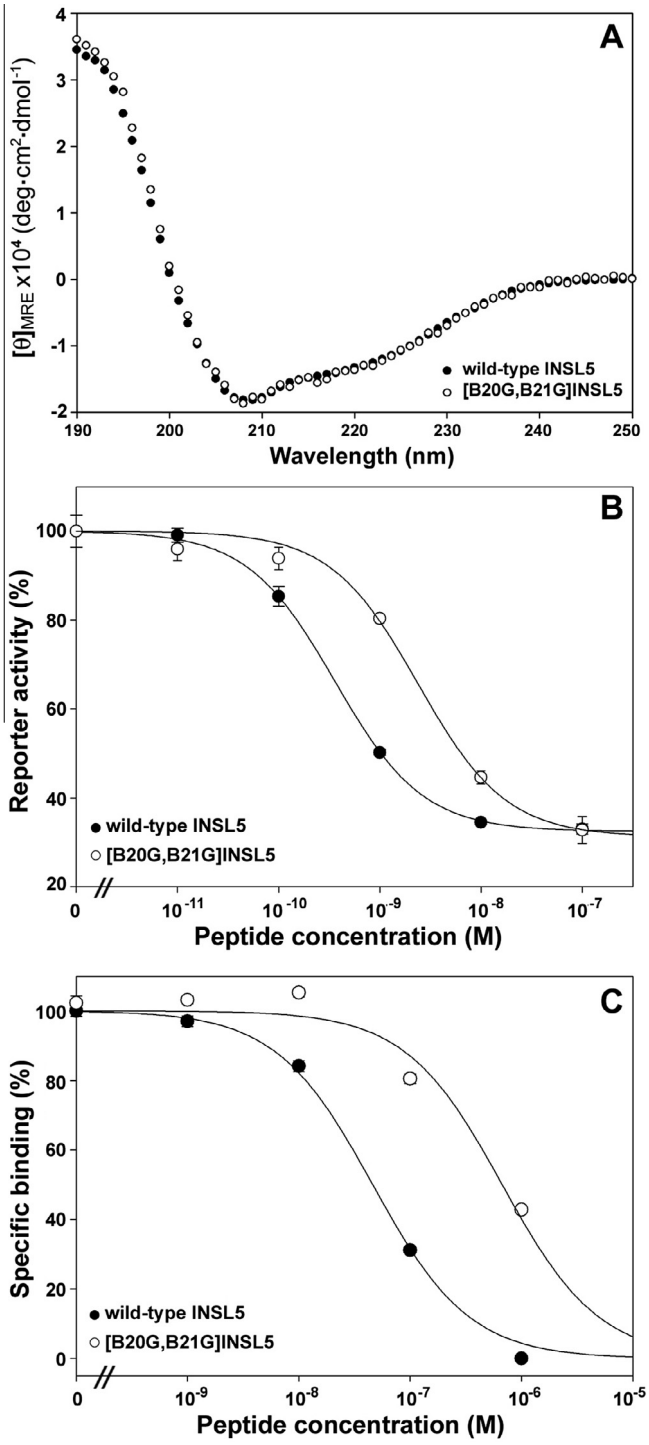

Fig. 5. Characterization of the mutant INSL5 carrying the B-chain C-terminal mutations. (A) Circular dichroism spectra. (B) Activation of the wild-type RXFP4. A CRE-controlled nanoluciferase was used as the reporter. The relative reporter activities were expressed as mean ± SE ($n = 3$) and fitted with sigmoidal curves using SigmaPlot 10.0 software. (C) Binding with the wild-type RXFP4. A europium-labeled R3/I5 peptide was used as the tracer. The specific binding data were expressed as mean ± SE ($n = 3$) and fitted with sigmoidal curves using SigmaPlot 10.0 software.

ligand–receptor interaction. Interestingly, [B23E]INSL5 had a higher activation potency towards [D104R]RXFP4 than towards wild-type RXFP4 (Table 3, row comparison), suggesting that Arg replacement of Asp104 partially rescued RXFP4 activity loss towards [B23E]INSL5. Thus, we deduced that B23Arg of INSL5 probably also interacted with Asp104 of RXFP4. For [E182R]RXFP4, [B13E]INSL5 showed a similar activation potency towards it compared with wild-type RXFP4 (Table 3, row comparison); by contrast, wild-type INSL5 showed an about 10-fold activity decrease towards [E182R]RXFP4 compared with wild-type RXFP4 (Table 3, row comparison). Thus, Arg replacement of Glu182 partially rescued the activity loss of RXFP4 towards [B13E]INSL5, suggesting that B13Arg of INSL5 likely also interacted with Glu182 of RXFP4. [E100R]RXFP4 could not be activated by the wild-type or mutant INSL5s (Table 3). Thus, we could not detect activity complementation between this mutant receptor with a mutant INSL5. Compared with the interaction of relaxin-3 with RXFP4, it was plausible to deduce that B23Arg of INSL5 also interacted with Glu100 of RXFP4, although the interaction could not be detected by the present approach. In summary, we propose the following probable electrostatic interactions between INSL5 and RXFP4: the B-chain central B13Arg of INSL5 interacts with both Asp104 and Glu182 of RXFP4; the B-chain C-terminal B23Arg interacts with both Glu100 and Asp104 of RXFP4.

Comparison of the electrostatic interactions of INSL5 and relaxin-3 with RXFP4 and the importance of the B-chain C-terminal conformation

Both INSL5 and relaxin-3 can bind and activate receptor RXFP4. As revealed by our present and previous studies, electrostatic interactions are used by both ligands to bind and activate receptor RXFP4, primarily involving the highly conserved positively charged B-chain Arg residues of the ligand and a highly conserved negatively charged EXXXD motif of the receptor. However, the electrostatic interactions between INSL5 and RXFP4 had subtle differences compared with those between relaxin-3 and RXFP4. For example, the B-chain C-terminal B23Arg of INSL5 probably interacts with both Asp104 and Glu100 of RXFP4; in contrast, the corresponding B-chain C-terminal B26Arg of relaxin-3 only interacts with Glu100 of RXFP4. This difference seems to be related to the different conformations of their B-chain C-termini. The B-chain C-terminal B23-B24 positions of relaxin-3s from different species are almost always occupied by small highly flexible Gly residues, resulting in a flexible B-chain C-terminus in relaxin-3 [13]. Thus, B26Arg of relaxin-3 was able to insert into a deeper position adjacent to Glu100, but far from Asp104 of RXFP4. Consequently, B26Arg of relaxin-3 only interacted with Glu100 of RXFP4. In contrast, larger residues almost always occupy the corresponding B-chain C-terminal positions (B20-B21) of INSL5s, typically an Ala-Ser dipeptide (Fig. 1B), resulting in a rigid α-helical conformation at the B-chain C-terminus of INSL5 [14]. Thus, B23Arg of INSL5 could only insert into a shallow position between Asp104 and Glu100 of RXFP4, and consequently was able to interact with both Asp104 and Glu100 of RXFP4. In our previous work, we demonstrated that a flexible B-chain C-terminus is important for relaxin-3 to efficiently interact with both RXFP4 and RXFP3 [10]. In the present work, we replaced the B-chain C-terminal Ala-Ser dipeptide (B20-B21) of human INSL5 with the corresponding Gly-Gly dipeptide of human relaxin-3. The mutant INSL5 was recombinantly expressed in *E. coli* as a single-chain precursor and refolded in vitro normally. After being enzymatically converted to the two-chain form, the mutant INSL5 had the correct molecular mass, as analyzed by mass spectrometry (Table 2). As analyzed by circular dichroism (Fig. 5A), the spectrum of the mutant INSL5 was quite similar to that of the wild-type INSL5, suggesting that the mutant INSL5 retained a native fold with correct disulfide linkages. Although the mutant INSL5 retained a native fold, it showed decreased activity towards its receptor RXFP4 in both the receptor-binding assay and the receptor-activation assay (Fig. 5B–C). Thus, a rigid α-helical conformation at the B-chain C-terminus was important for INSL5 to efficiently interact with its receptor RXFP4. Together with our

previous results [10], we concluded that INSL5 and relaxin-3 have different B-chain C-terminal conformation preferences for efficient interaction with receptor RXFP4.

Acknowledgements

This work was supported by grants from the National Natural Science Foundation of China (31270824, 30970609), the National Basic Research Program of China (973 Program, No. 2010CB912604), and the Fundamental Research Funds from Tongji University.

References

[1] R.A. Bathgate, M.L. Halls, E.T. van der Westhuizen, G.E. Callander, M. Kocan, R.J. Summers, Physiol. Rev. 93 (2013) 405–480.
[2] F. Shabanpoor, F. Separovic, J.D. Wade, Vitam. Horm. 80 (2009) 1–31.
[3] D. Conklin, C.E. Lofton-Day, B.A. Haldeman, A. Ching, T.E. Whitmore, S. Lok, S. Jaspers, Genomics 60 (1999) 50–56.
[4] S.Y. Hsu, Mol. Endocrinol. 13 (1999) 2163–2174.
[5] C. Liu, C. Kuei, S. Sutton, J. Chen, P. Bonaventure, J. Wu, D. Nepomuceno, F. Kamme, D.T. Tran, J. Zhu, T. Wilkinson, R. Bathgate, E. Eriste, R. Sillard, T.W. Lovenberg, J. Biol. Chem. 280 (2005) 292–300.
[6] C. Liu, J. Chen, S. Sutton, B. Roland, C. Kuei, N. Farmer, R. Sillard, T.W. Lovenberg, J. Biol. Chem. 278 (2003) 50765–50770.
[7] O. Burnicka-Turek, B.A. Mohamed, K. Shirneshan, T. Thanasupawat, S. Hombach-Klonisch, T. Klonisch, I.M. Adham, Endocrinology 153 (2012) 4655–4665.
[8] R.A. Bathgate, M.H. Oh, W.J. Ling, Q. Kaas, M.A. Hossain, P.R. Gooley, K.J. Rosengren, Front. Endocrinol. (Lausanne) 4 (2013) 13.
[9] W.J. Zhang, X.Y. Wang, Y.Q. Guo, X. Luo, X.J. Gao, X.X. Shao, Y.L. Liu, Z.G. Xu, Z.Y. Guo, Amino Acids 46 (2014) 1393–1402.
[10] X.Y. Wang, Y.Q. Guo, W.J. Zhang, X.X. Shao, Y.L. Liu, Z.G. Xu, Z.Y. Guo, FEBS J. 281 (2014) 2927–2936.
[11] X. Luo, R.A. Bathgate, W.J. Zhang, Y.L. Liu, X.X. Shao, J.D. Wade, Z.Y. Guo, Amino Acids 39 (2010) 1343–1352.
[12] W.J. Zhang, Q. Jiang, X.Y. Wang, S. Geng, X.X. Shao, Z.Y. Guo, J. Pept. Sci. 19 (2013) 350–354.
[13] K.J. Rosengren, F. Lin, R.A. Bathgate, G.W. Tregear, N.L. Daly, J.D. Wade, D.J. Craik, J. Biol. Chem. 281 (2006) 5845–5851.
[14] L.M. Haugaard-Jönsson, M.A. Hossain, N.L. Daly, D.J. Craik, J.D. Wade, K.J. Rosengren, Biochem. J. 419 (2009) 619–627.